Geosci. Model Dev. Discuss., 7, 3265–3305, 2014
www.geosci-model-dev-discuss.net/7/3265/2014/
doi:10.5194/gmdd-7-3265-2014

Geoscientific Model Development Discussions
Open Access

MATCH–SALSA – Multi-scale Atmospheric Transport and CHemistry model coupled to the SALSA aerosol microphysics model – Part 1: Model description and evaluation

C. Andersson[1], R. Bergström[1,2], C. Bennet[1], L. Robertson[1], M. Thomas[1], H. Korhonen[3,*], K. E. J. Lehtinen[3,4], and H. Kokkola[3]

[1]Swedish Meteorological and Hydrological Institute, 60176 Norrköping, Sweden
[2]University of Gothenburg, Department of Chemistry and Molecular Biology, 41296 Göteborg, Sweden
[3]Finnish Meteorological Institute, Kuopio Unit, P.O. Box 1627, 70211 Kuopio, Finland
[4]University of Eastern Finland, Department of Applied Physics, P.O. Box 1627, 70211 Kuopio, Finland
[*]now at: Finnish Meteorological Institute, Climate Research, P.O. Box 503, 00101 Helsinki, Finland

Received: 28 March 2014 – Accepted: 28 April 2014 – Published: 8 May 2014

Correspondence to: C. Andersson (camilla.andersson@smhi.se)

Published by Copernicus Publications on behalf of the European Geosciences Union.

Abstract

We have implemented the sectional aerosol dynamics model SALSA in the European scale chemistry-transport model MATCH (Multi-scale Atmospheric Transport and Chemistry). The new model is called MATCH–SALSA. It includes aerosol microphysics, with several formulations for nucleation, wet scavenging and condensation.

The model reproduces observed higher particle number concentration (PNC) in central Europe and lower concentrations in remote regions. The model PNC size distribution peak occurs at the same or smaller particle size as the observed peak at five measurement sites spread across Europe. Total PNC is underestimated at Northern and Central European sites and accumulation mode PNC is underestimated at all investigated sites. On the other hand the model performs well for particle mass, including secondary inorganic aerosol components. Elemental and organic carbon concentrations are underestimated at many of the sites.

Further development is needed, primarily for treatment of secondary organic aerosol, both in terms of biogenic emissions and chemical transformation, and for nitrogen gas-particle partitioning. Updating the biogenic SOA scheme will likely have a large impact on modeled $PM_{2.5}$ and also affect the model performance for PNC through impacts on nucleation and condensation. An improved nitrogen partitioning model may also improve the description of condensational growth.

1 Introduction

The demand for improved representation of aerosols in atmospheric models has increased during recent years. Most aerosol properties relevant to climate are both size and chemical composition dependent – thus there is a need to resolve the particle mass, number and chemical composition distributions in climate models (e.g. Chen and Penner, 2005; Roesler and Penner, 2010). Further, aerosol particles have adverse effects on human health (e.g. Pope and Dockery, 2006) which also are size and chemical composition dependent. Especially ultrafine particles (with diameter less than 100 nm) may be of particular importance for the health impacts (e.g. Oberdörster et al., 1995; Peters et al., 1997). The ultrafine particles do not contribute significantly to the particle mass concentration (PM) but they constitute a large proportion of the particle number concentration (PNC). As the dynamics of especially these ultrafine particles is very sensitive to the various aerosol microphysical processes, they need to be considered as high detail as possible in order to describe PNC accurately (e.g. Adams and Seinfeld, 2002). For chemical transport models (CTMs), which are used for predicting health impacts of regional or global particle concentrations, such detail may be even more crucial than for climate models.

CTMs that are commonly used for simulating atmospheric chemistry in Europe were recently reviewed by Kukkonen et al. (2012), with a previous version of our CTM MATCH as one of the models included in the study. The aerosol descriptions in such models can be classified in three main categories: bulk schemes, modal schemes and sectional schemes. In bulk schemes, typically the total mass concentration of particles, or the mass in a certain size interval is modeled – which has been a method of choice in MATCH (before the present work). In modal schemes, the aerosol size distribution is represented with a small number of modes, typically assuming lognormal size distribution shapes for the modes. The sectional scheme, in which the size distribution is represented by a large number of discrete bins, is the most accurate choice – but at the same time computationally the most expensive. E.g. PM-CAMx (Fountokis et al., 2011) and GLOMAP (Reddington et al., 2011) are examples of CTMs that have been successfully used for predicting PNC in Europe, which is also the focus of this work.

This is the first of two papers presenting a new aerosol dynamics version of a European scale Eulerian CTM; the new model is called MATCH–SALSA and was detailed in a SMHI RMK report (Andersson et al., 2013), which is included as Supplement to this paper. In this paper we highlight the main new features and present the results from evaluation tests. In a second paper (Andersson et al., 2014) results from various sensitivity tests, with the MATCH–SALSA model, will be presented. The aim of

MATCH–SALSA is to describe particle mass and number concentrations, and particle size distribution on the European scale. The new model features are developed with intention of coupling the model to climate models and radiative transfer calculations, and can also be utilized for the estimation of human exposure to particles.

2 Description of MATCH–SALSA

We have implemented the sectional aerosol dynamics model SALSA (Kokkola et al., 2008) in the European scale CTM MATCH (Multi-scale Atmospheric Transport and Chemistry; Robertson et al., 1999; Andersson et al., 2007). An earlier urban application of MATCH was applied to assess anthropogenic ultrafine particles in an urban environment (Gidhagen et al., 2005); seven monodisperse sizes were used and the aersosol dynamics considered water uptake, coagulation and dry deposition, but no nucleation or condensation processes. In earlier European scale MATCH versions (e.g. Robertson et al., 1999; Andersson et al., 2007, 2009), particles were handled with a simple bulk approach (with four size bins for primary particles), without any aerosol dynamics treatment (except hygroscopic growth in some model versions), but with dry and wet deposition of primary particles being dependent on particle size. The particle species considered were primary anthropogenic elemental carbon (EC), organic carbon (OC) and non-carbonaceous particles, as well as secondary inorganic aerosol (sulfate, nitrate, ammonium) and sea salt particles. Secondary organic aerosol was not included in the model. PNC was not described.

The coupling of SALSA to MATCH introduces a description of microphysics and particle aging in the model and makes it possible to describe PNC and the mixing state of the particles.

The layout of MATCH–SALSA is illustrated in Fig. 1. After initializations are completed the model iterates over time. The iterations are based on the meteorological time step (dtmet) where weather data are read or interpolated, new emissions are emitted, and lateral and top boundary concentrations of chemical species are set. After this, the emissions are injected and model transport fluxes are calculated with the internal sub-stepping time steps. Subsequently, the model chemistry, aerosol microphysics and cloud droplet number concentrations are calculated. Meteorological data are read at regular intervals, typically every three or six hours. Boundary conditions may be updated at compound dependent intervals.

Natural and anthropogenic emissions are included in the model[1]. Sea salt and isoprene emissions are calculated online, whereas anthropogenic and other emissions (volcanic sulfur, marine DMS and biogenic monoterpenes) are given as input data to the model. All primary particle components are emitted both as mass and number. Sea salt emissions are modeled as described in Foltescu et al. (2005) but modified to allow arbitrary choice of size bins. For the smallest bins (diameter ≤ 1 µm) the description by Mårtensson et al. (2003) was used; for larger sizes the sea salt generation function was taken from Monahan et al. (1986). Biogenic emissions of isoprene are calculated using the E-94 isoprene emission methodology proposed by Simpson et al. (1995).

The transport model includes advective and turbulent transport. Particle number and mass are transported independently in MATCH–SALSA. The transport scheme is described in detail in Robertson et al. (1999).

2.1 Chemistry

The original MATCH photochemistry scheme (Langner et al., 1998) was, to a large extent, based on the EMEP MSC-W (European Monitoring and Evaluation Programme Meteorological Synthesizing Centre – West) scheme (Simpson, 1992; Simpson et al., 1993), but with an alternative treatment of isoprene chemistry, using an adapted version of the Carter 1-product mechanism (Carter, 1996; Langner et al., 1998). A simplified mixture of a dozen representative compounds ("lumped molecules") is used to model

[1]Note that in the present version of the model emissions from open fires (wildfires and agricultural burning) are not included.

GMDD
7, 3265–3305, 2014

all organic molecules emitted to the atmosphere (e.g., *o*-xylene represents all emitted aromatic species).

The gas-phase chemistry scheme in MATCH has remained mostly the same since 1998, but a number of reaction rates have been updated, taking into account new recommendations from IUPAC (Atkinson et al., 2006) and the Master Chemical Mechanism, MCM v3 (Jenkin et al., 1997; Saunders et al., 2003, via website: http://mcm.leeds.ac.uk/MCM); a few new gas phase components have also been added to the scheme. The revision of the MATCH chemistry scheme was based closely on the updates done in the EMEP MSC-W model, during 2008–2009, as documented by Simpson et al. (2012); the updated gas-phase reaction scheme in MATCH is mostly identical to the EMEP MSC-W EmChem09 scheme of Simpson et al. (2012), but for isoprene the scheme from Langner et al. (1998) is retained (with some reaction rates updated to IUPAC recommended values, Atkinson et al., 2006).

In addition to gas-phase chemistry, aqueous-phase oxidation of SO_2 in cloud water (based on Berge, 1992) and a few heterogeneous reactions for nitrogen compounds are included in the model. For MATCH–SALSA some further modifications related to particle formation have been made and the scheme used in the present work consists of approx 140 thermal, wet and photolysis reactions, including about 60 different chemical species.

The chemistry code includes a simple scheme for secondary organic aerosol (SOA) formation from biogenic monoterpene emissions; α-pinene is used as a surrogate. In the present study we assume rapid formation of condensable SOA after gas-phase oxidation of α-pinene (by O_3, OH or NO_3; oxidation rates are based on MCM v3.2, http://mcm.leeds.ac.uk/MCM); we assumed that 30 % (mass-based) of oxidized organics from all oxidation paths are SOA forming compounds so that they are available for the OM condensation scheme in SALSA. The high SOA-yield used here (30 %) is unrealistic for real α-pinene emissions; typical SOA-yields for this monoterpene in smog-chamber experiments are around 5 % (e.g., Mentel et al., 2009). Note that the simplified BSOA "scheme" used in the present study is only included to test the

GMDD
7, 3265–3305, 2014
MATCH–SALSA – Part 1: Model description and evaluation
C. Andersson et al.

organic-aerosol parts of MATCH–SALSA, with minimal changes to the standard photochemistry scheme; it is not expected to model BSOA formation in a very realistic way compared to real-world conditions but, given the high uncertainties in monoterpene emissions and the neglect of other BSOA-forming emissions, it was considered a reasonable approach for the development phase of MATCH–SALSA.

2.2 Aerosol microphysics

The SALSA model was designed to obtain a balance between computational efficiency and numerical accuracy. This was reached by keeping the number of tracer variables low by using a relatively coarse particle size resolution and including only the relevant chemical compounds in different particle size ranges (see Kokkola et al., 2008). The size resolution is varying across the size spectrum with higher resolution for particles that are crucial in cloud activation and for aerosol radiative properties. Aerosol number and mass concentrations are described by three size ranges, divided into size bins with a constant internal volume ratio. The number of bins in each range and the size limits of the size ranges are flexible. In addition, the chemical compounds are that are treated in each size range are chosen dependent on the compounds that are relevant to that size of particles in the real atmosphere. The first size range (nucleation and Aitken modes) includes sulfate (SO_4^{2-}) and OC, the second (accumulation mode) and third (coarse mode) size ranges includes SO_4^{2-}, EC, OC, sea salt (NaCl) and mineral dust. SO_4^{2-} and OC are combined to calculate the water soluble fraction of the particles in the third size range, whereas sea salt retains one fraction of the third range of its own. The hygroscopicity of the aerosol is calculated using the Zdanowskii–Stokes–Robinson method (Jacobson, 2002).

At the end of each microphysical time step the size distribution is updated to take into account growth or shrinkage of particles due to dynamic and chemical transformation processes. Particulate nitrogen species are described by a simplified chemistry scheme and currently handled outside SALSA. Ammonium bound to sulfate was distributed according to the sulfate on particle sizes. Ammonium nitrate was distributed according to the aerosol surface distribution and coarse nitrate was treated separately.

In this study nucleation is simulated through an activation type nucleation formulation (Kulmala et al., 2006; Riipinen et al., 2007) and the formation rate of 3 nm particles (J3) is calculated according to Lehtinen et al., 2007. Nucleation is solved concurrently with condensation using the methodology of Jacobson (2002). This methodology takes into account the competition of nucleation and condensation in the mass transfer of volatile species between gas and particle phase. The model also includes other nucleation scheme options for example binary nucleation (Vehkamaki et al., 2002), ternary nucleation (Napari et al., 2002a, b) and activation of both H_2SO_4 and organic vapors (Paasonen et al., 2010). Tests of these alternative nucleation schemes will be presented in the companion paper (Andersson et al., 2014).

The scheme used for gas-to-particle transformation is the Analytical Predictor of Condensation scheme with saturation vapor pressure set to zero (Jacobson, 1997). The method solved non-equilibrium transfer of semi-volatile compounds between gases and particles over a discrete time step. Since it requires no iteration, is mass conserving, and has been shown to be accurate over time step length of 7200 s (Jacobson, 2005) it is very well suited for large scale atmospheric models such as MATCH.

Coagulation is described using a semi-implicit scheme (Jacobson, 1994). Similarly to the condensation scheme, a semi-implicit coagulation scheme does not require iteration and is mass conserving. Since coagulation is computationally the most time consuming microphysical process, coagulation between aerosol pairs for which coagulation efficiency is low are not taken into account. The detailed list of selected collision pairs accounted for in the coagulation routine is given in Kokkola et al. (2008).

Further details of the SALSA model is given by Kokkola et al. (2008) and Bergman et al. (2012).

2.3 Deposition

Dry deposition of trace gases are calculated with a simple resistance approach (Chamberlain and Chadwick, 1965) that is dependent on land use and season. Wet scavenging of most gaseous species is proportional to the precipitation intensity. For ozone, hydrogen peroxide and sulfur dioxide in-cloud scavenging is calculated using Henry's law equilibrium; sub-cloud scavenging is neglected for these species. Wet and dry deposition of gases is described in detail by Andersson et al. (2007).

Particle dry deposition is calculated using a scheme based on Zhang et al. (2001), (including hygroscopic growth) adapted to a smaller set of land use classes (Water, Forest, Low vegetation and No vegetation). More details on dry deposition of *particle* species are given in the Supplement.

Particles are wet deposited through incloud (W_{IC}) and subcloud (W_{SC}) scavenging. The incloud scavenging in the model depends on the fraction of cloud water or ice that is precipitated in each grid box, the fraction of each particle size bin that are inside the cloud droplets, the fraction of the box that is covered by cloud and the concentration of particles.

In MATCH–SALSA the fraction of particles that are inside the cloud droplets is assumed to be the fraction of particles that are activated as cloud droplets. A simplified scheme can be used for this fraction, where the fraction of the particles is parameterized following Seinfeld and Pandis (1997). This means that in-cloud particles larger than 80 nm in diameter will be activated as cloud droplets. This latter description was used in this study and it is a simplification; in reality the activated fraction depends on meteorological conditions.

A more advanced formulation, which is more CPU-time consuming, is also implemented in the model. MATCH–SALSA model can be run coupled to an online cloud activation model that computes cloud droplet number concentrations based on the prognostic parameterization scheme of Abdul-Razzak and Ghan (2002). The number of particles activated to cloud droplets in each size section is determined by the particle

GMDD
7, 3265–3305, 2014

size distribution, their number concentration and chemical composition as well as the updraft velocity and the maximum supersaturation of the air parcel. Running the model with particle activation is optional. There is an option to use the resulting activated particle fraction in each size bin for calculation of incloud scavenging of particles. In this formulation the parameter F_s is calculated in each time step for each grid point, here F_s is the activated fraction of each particle class.

The subcloud scavenging in the model is treated in a similar way as by Dana and Hales (1976). In MATCH–SALSA, a simplified approach is used where a monodisperse washout coefficient is calculated for each particle bin and a standard rain drop spectrum[2] is assumed for all precipitation. The washout coefficient (i.e., the fraction of a species that is removed by precipitation below clouds) depends on precipitation amount and takes into account particle collection by Brownian diffusion, inertial impaction and interception. The total wet deposition is the sum of the incloud and subcloud scavenging.

Alternatively, more parameterized formulations for the particle wet scavenging can also be used. Further details on the wet scavenging of particles are given in the Supplement and in the companion paper Andersson et al. (2014).

3 Model set up

In this section we describe the setup of the simulation used to evaluate MATCH–SALSA in this paper.

Meteorology is input at regular time intervals; here we used three-hourly fields from the HIRLAM (Hi-Resolution Limited-Area Model; Undén et al., 2002) weather forecast model. The input meteorology is interpolated to hourly resolution. The model set up covers Europe with a spatial resolution of approx 44 km. The lowest model level is

[2] A representative frontal rain spectrum is used, $R_g = 0.02$ cm, $\Sigma_g = 1.86$ (Dana and Hales, 1976).

GMDD
7, 3265–3305, 2014

approx 60 m thick and in total 22 vertical levels are used; the top level is at approx 5 km height.

For the aerosol size distribution the following settings were used (see Fig. 2): the first subrange covered the diameter interval 3–50 nm, with three log-normally distributed size bins; the second subrange covered the diameter interval 50–700 nm, with four bins each for soluble and insoluble particle types; the third subrange covered the diameter size range 700 nm–10 µm, with three size bins for each of the following three particle types: seasalt, soluble and insoluble.

The top and lateral boundary concentrations of gaseous and particle species, including seasonal variation for some species, were set as described in Andersson et al. (2007). However, OM boundary concentrations on the southern, western and northern boundary were set based on marine OM measurements (O'Dowd et al., 2004).

Monthly biogenic emissions of monoterpenes were taken from the EMEP MSC-W model (Bergström et al., 2012; Simpson et al., 2012). α-pinene is used here as a surrogate species for all biogenic monoterpenes. The anthropogenic emissions of gass and primary aerosols are taken from the TNO-MACC emission inventory (Kuenen et al., 2011; Pouliot et al., 2012; see also the MACC – Monitoring the Atmospheric Composition and Climate – project web page http://www.gmes-atmosphere.eu/). The TNO-MACC emissions are given as annual totals; seasonal, weekday and diurnal variations of the emissions are based on results from the GENEMIS project (http://genemis.ier.uni-stuttgart.de/; Friedrich and Reis, 2004). The particle emissions of EC and OM[3] were distributed over different particle sizes according to sector resolved mass size distributions described by Visschedijk et al. (2009). The emissions of oxidized sulfur (SO_x) were split into 99 % SO_2 and 1 % H_2SO_4. The distribution of SO_x emissions between SO_2 and more oxidized compounds was discussed by Spracklen et al. (2005); the fraction of SO_2 increases with grid resolution and is typically set

[3]OM emissions are assumed to be distributed over different particle sizes in the same way as OC.

GMDD
7, 3265–3305, 2014

to between 95–100 % in European scale models. The emitted sulfate mass was distributed over particle sizes in the same manner as OM. NOx and NMVOC were emitted as in Andersson et al. (2007).

4 Evaluation of MATCH–SALSA

4.1 Measurement data

The measurement data that were used to evaluate the PNC size distribution, particle mass ($PM_{2.5}$ and PM_1), EC and OC were extracted from EBAS (http://ebas.nilu.no). Details of the stations used in the evaluation of particle number size distribution, PM_1, $PM_{2.5}$, EC and OC are given in the Supplement (Table 5). Secondary inorganic aerosol (SIA) species were evaluated against available measurements in the EMEP network for 2007.

For evaluating PNC, five stations from EBAS were chosen to represent different parts of Europe; all classified as rural background sites. Two of the measurement sites: Melpitz (in eastern Germany) and K-Puszta (in central Hungary), are relatively close to regions with large emissions. Hyytiälä (in the inland of southern Finland) and Aspvreten (ca. 70 km south west of Stockholm, in south eastern Sweden) were chosen as regional background stations occasionally impacted by aged particles due to transport from large emission sources in Europe. Mace Head was chosen to represent clean marine conditions; episodic influences from continental Europe or emissions from the British Isles can also be seen at this site.

4.2 Model evaluation of PNC

Figure 3 shows the modeled annual mean PNC in Europe; both total PNC (Fig. 3a) and the PNC in the different model size bins up to 700 nm are shown (Fig. 3b–g). Corresponding measured annual mean PNC at the five observation sites are also displayed in circles for particle sizes where measurements are available.

GMDD
7, 3265–3305, 2014

The largest modeled total PNC (Fig. 3a) are found in areas with high SO_x emissions (e.g., areas around large point sources in Spain, Poland, south-eastern Europe, the Ukraine, Russia and the area around Etna; as well as along shipping routes around the Iberian Peninsula and the Gibraltar strait). These results are in line with other model studies (e.g. Yu and Luo, 2009; Spracklen et al., 2010; Ahlm et al., 2013).

Most of the total PNC in the model resides in the Aitken mode bins (particle diameters 7–20 nm and 20–50 nm; Fig. 3c and d). The highest PNC in the smallest bin (Fig. 3b), indicating recent nucleation, are found in urban areas in Russia and Belarus. Increased values in this bin are also seen along the shipping lanes, as a result of relatively clean air combined with emissions. The Aitken mode PNC pattern (Fig. 3c and d) is similar to the total PNC distribution (Fig. 3a), and the highest concentrations are found in areas in Spain, Turkey, Former Yugoslavia, Bulgaria, and north-eastern Russia, and around the volcano Etna. The highest accumulation mode (50–700 nm) PNC (Fig. 3e–h) are found in southern Europe. This is partly due to relatively large emissions of primary fine particles and gaseous SO_x, and partly due to less precipitation in southern Europe compared to the north and west allowing accumulation mode particles to reside longer in the atmosphere.

4.2.1 Overall performance

We evaluate the model performance (see Figs. 4–6) in terms of total and accumulation mode particle number concentration (PNC and PNC_a, respectively) against the five European surface sites (see also the Supplement). Due to differences in emissions and atmospheric processes between the seasons, we separate performance during summer half-years (April–September) from winter (October–March). For example, residential biomass burning emissions are much higher during winter than during summer, while biogenic VOC emissions are largest during summer. Both these sources are associated with large uncertainties regarding the emissions and modeling. It should be noted that the size ranges for PNC and PNC_a vary between the stations depending on the measurement interval.

GMDD
7, 3265–3305, 2014

4.2.2 Spatial distribution

Modeled total PNC shows, is general, moderate to poor agreement with the observations (Fig. 4a). At most sites the deviation between observed and modeled mean is large both in summer and winter, and the correlation coefficients for daily mean PNC are low (0.05–0.66). The relatively poor agreement between model and observations is not unexpected considering the coarse resolution of the model.

The model captures the general features of lower total and accumulation mode PNC in the northern and north-western parts of Europe (Fig. 3). Aspvreten and Mace Head have the lowest modeled and observed PNCs (Fig. 4a). However, looking in more detail at the stations (Fig. 4) there are some discrepancies.

Melpitz has the clearly highest observed total PNC (during both winter and summer; Fig. 4a); the model severely underestimates the PNC at Melpitz and predicts much higher total PNC in K-Puszta than in Melpitz. The highest *observed* accumulation mode PNCs are found at K-Puszta and Melpitz (the PNC are at similar levels for both seasons and both sites; Fig. 4b); just as for total PNC, the model predicts much higher accumulation mode PNC at K-Puszta than at Melpitz.

Thus the spatial distribution of PNC in the model is not in perfect agreement with the observations. There may be many reasons for this. One important reason for the high modeled total PNC at K-Puszta is the high rate of nucleation which is caused by the large emissions of SO_x in the area.

4.2.3 Size distribution

The modeled and observed size distributions at all five stations are shown in Fig. 5. A common feature for the PNC size distribution is that PNC are underestimated or on the same level as the measurements, except for the smallest sizes at K-Puszta (Fig. 5d) and Mace Head (Fig. 5e), which are overestimated both during winter and summer. At these sites the accumulation mode is underestimated, whereas the mean total PNC is overestimated or close to the observed. Overall, at all stations, the shape

GMDD
7, 3265–3305, 2014

of the size distribution is captured well, but during winter at K-Puszta (Fig. 4d), during summer at Aspvreten (Fig. 4a) and Hyytiälä (Fig. 4b), and the whole year at Mace Head (Fig. 4e) there is a shift of the distribution peak to smaller sizes in the model than in the observations. The reason for the maximum occurring at too small sizes may be too little condensation onto nucleating particles in the model.

4.2.4 Temporal evolution

Figure 6 shows the modeled and observed temporal variation of the daily mean PNC at the five sites. New particle formation is evident in the model in the form of peaks in the very smallest particles sizes. These coincide with the observed maximum total PNC on some occasions, sometimes there is a shift of a few days. Especially at Hyytiälä (Fig. 6a), Aspvreten (Fig. 6b) and Melpitz (Fig. 6c), there are peaks in the observations when there are none in the model. This illustrates that nucleation is a difficult process to capture in the model; one reason for this is the coarse scale of the model – each grid cell is representative of a large area (ca. 2×10^3 km^2). Furthermore wintertime nucleation peaks in the observations are probably of local origin that can not be captured by a regional scale CTM.

The best correlation between modeled and observed PNC is found at Melpitz (r = 0.70; Fig. 6c and f) but the model underestimates PNC most of the time; observed PNC is almost always high at this site. At Mace Head (Fig. 6e) some of the observed peaks are fairly well modeled but the overall correlation coefficient is modest (r = 0.46; Fig. 6f); the timing of some peaks is shifted in the model compared to the observations and some model peaks are not seen in the observations and vice versa. The model grossly overestimates the total PNC at K-Puszta (Fig. 6d) during summer, but the temporal variation for particles sizes > 20 nm follows the measurements fairly well; during winter the model PNC is in better agreement with the observations. At Hyytiälä (Fig. 6a) a lot of nucleation is observed; this is not captured by the model, possibly because of the lack of organic nucleation in this simulation as shown in Andersson et al. (2014).

4.3 Model evaluation of particle mass and composition

Simulated annual average total PM_{10}, and the chemical components that constitute PM_{10}, are displayed in Fig. 7. The largest concentrations of PM_{10} (Fig. 7a) are found at anthropogenic emission hotspots (e.g., northern Italy, Moscow and the eastern Ukraine) and over the Atlantic Ocean and parts of the Mediterranean Sea. The highest modeled concentrations over land are due to large anthropogenic emissions of primary anthropogenic inorganic aerosol (DUST; Fig. 7d), except in northern Italy, where there is a large contribution from ammonium nitrate, and in southeastern Europe, and some sulfur emission hotspots, where sulfate (Fig. 7e) dominates PM_{10}. Over the oceans (and in large parts of western and northern Europe), the largest contribution to PM_{10} is from sea salt particles (Fig. 7h); important sulfate contributions are also seen, especially around Etna and the eastern Mediterranean Sea. OM (Fig. 7c) gives the largest modeled non-sea salt contributions to PM_{10} in parts of southern/western Europe and in the Nordic region. In following subsections we present evaluation statistics for the different particle components.

4.3.1 Secondary inorganic aerosol (SIA)

Statistics from the evaluation for SIA components (particulate sulfate, SO_4^{2-}; nitrate, NO_3^-; and ammonium, NH_4^+) are shown in Table 1 and in the Supplement: Tables A15–A19 and Figs. A32–A36. In order to avoid biases due to possible incorrect separation of gas and particle phase nitrogen in the measurements, we also include evaluation results for total nitrate (TNO_3: $HNO_3(g) + NO_3^-(p)$) and total reduced nitrogen (TNH_x: $NH_3(g) + NH_4^+(p)$).

Sulfate has a low mean bias (4 %) whereas the root mean square error normalized to the observed mean (CV(RMSE)) is around 50 %. The average (Pearson) correlation coefficient (mean r) based on daily means at the included sites is 0.52 and the spatial correlation coefficient (for the annual mean concentration at the stations, spatial r) is 0.57. The model performance for the nitrogen compounds (NO_3^-, $HNO_3 + NO_3^-$, NH_4^+

and NH_x) at individual stations is of similar quality to that of sulfate. The model underestimates the concentration of the nitrogen components by about 10–20 %, while the CV(RMSE)s in most cases are a bit lower than for sulfate (range from 36 to 49 % for the N-components). The mean r vary between 0.44 and 0.59, whereas the spatial r are higher (between 0.79 and 0.87).

4.3.2 Elemental and organic carbon

While the atmospheric observation measure organic carbon (OC), the model describes organic matter (OM). In the evaluation we assume a OM : OC ratio of 1.4. The actual ratio varies with location and season (e.g., Simon et al., 2011) and is usually between 1.25 and 2.5, with a greater ratio for more aged OM (Turpin et al., 2000; Kupiainen and Klimont, 2007; Aiken et al., 2008). Thus, the choice of a fixed OM : OC ratio will lead to model under- or overestimation depending on measurement site and time of year. Figure 8 shows the annual observed and modeled mean concentrations of EC (Fig. 8a and b) and OC (Fig. 8c and d) at individual measurement sites, as well as the associated daily correlation coefficients; the Supplement contains detailed results for EC and OC in Table A20 and time series plots in Figs. 15, A37, and A38.

Both EC and OC are underestimated at many of the sites. The underestimation is especially large at the Italian sites and Payerne (Switzerland) during winter for both EC (Fig. 8b) and OC (Fig. 8d), and for EC at Melpitz (Fig. 8a and b). There is a generally higher correlation for EC than OC; OC is more complicated to model than EC, since it is a combination of primary and secondary components, many of them semi-volatile. The reasons for the model – measurement differences are likely to vary between seasons and locations; e.g., wintertime emissions from residential combustion are often underestimated (e.g. Simpson et al., 2007; Gilardoni et al., 2011; Bergström et al., 2012), during the summer half-year biogenic VOC emissions and wildfires may be more important sources of carbonaceous particles.

GMDD
7, 3265–3305, 2014

4.3.3 Total particulate matter (PM_1 and $PM_{2.5}$)

Evaluation of PM_1 and $PM_{2.5}$ at 28 measurement sites is presented in Fig. 9. and in the Supplement Table A21 and Fig. A39; detailed time series plots are given in the Supplement Figs. 17, A40 and A41. For PM_1 the annual means at the sites with the lowest concentration (Scandinavian sites NO01, FI17, DK41) are overestimated by the model. On the other hand, at the central European sites the PM_1 concentrations are much better captured. The model underestimates $PM_{2.5}$ by 14 % (spatial average) and the spatial correlation coefficient is 0.64. Out of the 35 evaluated annual means (PM_1 and $PM_{2.5}$) at the 28 stations, six means (at five stations) deviate by more than 50 %. The largest underestimations of $PM_{2.5}$ are seen at the measurement sites with the highest observed annual mean. The underestimation of $PM_{2.5}$ can be due to a number of reasons including underestimated emissions, too short aerosol lifetime or too little secondary aerosol production. There is probably too little EC and OC in the model, at least at some of the sites, which can be explained by underestimated emissions.

5 Identified issues

During this work we found that further improvement is needed for a better representation of PNC. Here, in this section we would try to address some of the issues related to model development and measurements that could be relevant. The three of these issues will be further investigated in Andersson et al. (2014):

– *Distribution of SO_x*. In atmospheric models, given fractions of SO_x emissions are assumed as gaseous SO_2, H_2SO_4 and primary sulfate, which is intended to account for subgrid scale processes of gas phase transformation and gas-to-particle partitioning. The assumed fractions have large uncertainty and it is not clear from the literature how to divide SO_x emissions between SO_2(g), H_2SO_4(g) and particulate sulfate in modeling studies. Spracklen et al. (2005) discussed that the distribution depends on model resolution. Lee et al. (2013) have shown that the sub-grid production of a few per cent mass of sulfate particles in plumes is much more important for CCN uncertainty than the SO2 emissions themselves. Since we suspect this choice to have impact on the model results, we investigate this further in Andersson et al. (2014).

- *SOA condensation and nucleation.* This version of MATCH–SALSA contains a scheme of formation of SOA, in which SOA precursors are assumed to condense on particles as non-volatile compounds. The SOA formation scheme is simplified and needs further development. For example, atmospheric SOA compounds have a wide variety of volatilities that would affect their partitioning between gas and particles. Also, biogenic emissions are highly uncertain, and the chemistry of SOA formation is complex and modelling of SOA is fraught with great difficulty (e.g. Hallquist et al., 2009; Bergström et al., 2012). For these reasons we test the model sensitivity on the amount of SOA available for condensation in Andersson et al. (2014). Further, MATCH–SALSA contains a scheme including organic nucleation that was not used in this study. In Andersson et al. (2014) the impact of including organic nucleation on modeled PNC is also tested.

- *Wet scavenging* is the most important sink for accumulation mode particles. At many sites particle concentrations are underestimated by the MATCH–SALSA model when the standard wet deposition scheme is used. Several other, more and less advanced, formulations of wet scavenging are implemented in the MATCH model and in the companion paper we also investigate the sensitivity of the of the modeled particle mass and PNC on the wet scavenging formulation.

The treatment of sea spray needs to be further evaluated and the model scheme for sea salt particles may need to be updated. For PM_1 the annual means at the sites with the lowest concentration (Scandinavian sites NO01, FI17, DK41) are overestimated by the model. This seems to be partly due to overestimation of sea salt. Evaluation scores for modeled PM_1 and $PM_{2.5}$ excluding sea salt aerosol in the total PM mass (see Supplement Table A21, Figs. 18 and A39) gives higher correlation coefficients for

GMDD
7, 3265–3305, 2014

daily mean $PM_{2.5}$ or PM_1 at 22 of the 28 sites (and lower at only one site) than when sea salt is included. This is an indication of too much sea salt at the wrong time. It may be due to too strong sea salt emissions and/or too weak sink processes for the sea salt, since substantial improvements in correlation are seen also at some far inland sites.

For EC and OC, there is probably a combination of need for model development, uncertainties in measurements and emission inventories. At Ispra (IT04) in northern Italy, the model performs fairly well for carbonaceous aerosol during summer but greatly underestimates both EC and OC during wintertime (Fig. 8 and Supplement Fig. 15). One reason may be due to underestimation of residential wood combustion emissions (e.g. Bergström et al., 2012). The model also underestimates NO_2 (by 43 % in summer and 51 % in winter). Both the observations and the model results show a clear seasonal cycle with higher concentrations during winter for NO_2 as well as for EC and OC. However, for EC and OC the model underestimation during winter is much larger (−74 and −87 %, respectively) than during summer (−20 and −37 %, respectively) (Supplement Fig. 15). The poor model performance for EC and OC during winter is likely due to lacking emissions from one or more emission sectors, with greater emissions of EC and OC during winter, but relatively small contribution to NO_2. This work therefore supports the results of previous studies (e.g. Gilardoni et al., 2011) that have concluded that residential wood combustion emissions are likely underestimated in current emission inventories, at least in the area around Ispra.

For the German site Melpitz, the model grossly underestimates EC throughout the year (Supplement Fig. A37). OC is generally captured fairly well at the station, with underestimation of OC in $PM_{2.5}$ and PM_{10} (but not PM_1) during winter and overestimation for OC in $PM_{2.5}$ and underestimation (−25 %) in PM_{10} during summer (Supplement Fig. A38). Part of the reason for the relatively high EC measurements at Melpitz is that the measurement technique used at this site, to separate OC from EC, has no charring correction and is expected to lead to too high EC values and to underestimate OC (see Genberg et al., 2013, and references therein). There are large peaks during spring and late autumn of OC (and EC) in $PM_{2.5}$ and PM_{10}, which are clearly underpredicted.

The peak in the beginning of April coincides with a vegetation fire episode (Genberg et al., 2013); the earlier peaks and the late autumn peaks are perhaps more likely due to residential combustion or other missing/underestimated sources, possibly also due to eastern fire activities (Jönsson et al., 2013). Stern et al. (2008) compared five different chemical transport models to observations from northern and eastern Germany during highly polluted conditions. None of the models could reproduce the very high EC concentrations observed at Melpitz. Stern et al. (2008) suggested that the large underestimations of EC may be an indication that emissions in the central European region were underestimated during these episodes.

6 Conclusions

We have implemented the sectional aerosol dynamics model SALSA (Kokkola et al., 2008) in the European scale CTM MATCH (Multi-scale Atmospheric Transport and Chemistry; Robertson et al., 1999). The new model is called MATCH–SALSA. It includes aerosol microphysics with several options for nucleation, wet scavenging and condensation.

In general, the model reproduces observed lower particle number concentration (PNC) in northern and north-western Europe and remote regions. The model peak PNC occurs at the same or smaller particle size as the observed peak. Total PNC is underestimated at some sites. The model performs well for particle mass, including secondary inorganic aerosol components. Particulate elemental and organic carbon are underestimated at many of the sites.

The model can be used in applications knowing the restrictions of what the model manages well and what needs further improvements. Before using the model for simulating $PM_{2.5}$, the SOA formulation needs further improvements. MATCH–SALSA is computationally heavier than MATCH, which also puts restrictions on when the model can be used.

GMDD
7, 3265–3305, 2014

The development of the MATCH–SALSA model is continuing and in the near future focus will be on the following areas:

- An updated biogenic emission module is needed for realistic treatment of BSOA formation. Updating the biogenic SOA scheme will likely have a large impact on modeled $PM_{2.5}$ and also affect the model performance for total PNC through impacts on nucleation and condensation.
- Nitrogen gas-particle partitioning should be coupled to the microphysics. This may increase condensational growth, which is underestimated in the present version of the model.
- Open fire emissions from wildfires and agricultural activities (biomass burning) should be added to the model.
- Dust emissions from road traffic, agricultural activities and non-vegetated soils including desert areas should be included in the model.
- Processes affecting sea salt need further work and evaluation. This study has shown large modeled sea salt peaks that are not seen in the measurements. Both emissions and deposition of sea salt particles should be investigated.
- Emission inventories need to be improved, especially for EC and OC emissions.

Supplementary material related to this article is available online at http://www.geosci-model-dev-discuss.net/7/3265/2014/gmdd-7-3265-2014-supplement.pdf.

Acknowledgements. The work of developing and evaluating this new model was financed by the Swedish Environmental Protection Agency (Naturvårdsverket) through the Swedish Clean Air Research Programme (SCARP; http://www.scarp.se). We also acknowledge funding from the Swedish Research Council FORMAS under the MACCII project (No 2009-409) and from the Academy of Finland (decision: 250348).

GMDD
7, 3265–3305, 2014

References

Abdul-Razzak, H. and Ghan, S. J.: A parameterization of aerosol activation, 3. Sectional representation, J. Geophys. Res., 107, 4026, doi:10.1029/2001JD000483, 2002.

Adams, P. J. and Seinfeld, J. H.: Predicting global aerosol size distributions in general circulation models, J. Geophys. Res., 107, 4026, doi:10.1029/2001JD000483, 2002.

Ahlm, L., Julin, J., Fountoukis, C., Pandis, S. N., and Riipinen, I.: Particle number concentrations over Europe in 2030: the role of emissions and new particle formation, Atmos. Chem. Phys., 13, 10271–10283, doi:10.5194/acp-13-10271-2013, 2013.

Aiken, A. C., Decarlo, P. F., Kroll, J. H., Worsnop, D. R., Huffman, J. A., Docherty, K. S., Ulbrich, I. M., Mohr, C., Kimmel, J. R., Sueper, D., Sun, Y., Zhang, Q., Trimborn, A., Northway, M., Ziemann, P. J., Canagaratna, M. R., Onasch, T. B., Alfarra, M. R., Prevot, A. S. H., Dommen, J., Duplissy, J., Metzger, A., Baltensperger, U., and Jimenez, J. L.: O/C and OM/OC ratios of primary, secondary, and ambient organic aerosols with high-resolution time-of-flight aerosol mass spectrometry, Environ. Sci. Technol., 42, 4478–4485, doi:10.1021/es703009q, 2008.

Andersson, C., Langner, J., Bergström, R.: Interannual variation and trends in air pollution over Europe due to climate variability during 1958–2001 simulated with a regional CTM coupled to the ERA40 reanalysis, Tellus B, 59, 77–98, 2007.

Andersson, C., Bergström, R., and Johansson, C.: Population exposure and mortality due to regional background PM in Europe – long-term simulations of source region and shipping contributions, Atmos. Environ., 43, 3614–3620, 2009.

Andersson, C., Bergström, R., Bennet, C., Thomas, M., Robertson, L., Kokkola, H., Korhonen, H., and Lehtinen, K.: MATCH–SALSA – Multi-scale Atmospheric Transport and Chemistry model coupled to the SALSA aerosol microphysics model, SMHI RMK Report no 115, available at: http://www.smhi.se/publikationer/match-salsa-multi-scale-atmospheric-transport-and-chemistry-model-coupled-to-the-salsa-aerosol-microphysics-model-1.34623 (last access: 6 May 2014), 2013.

Andersson, C., Bergström, R., Bennet, C, Thomas, M., Robertson, L., Kokkola, H., Korhonen, H., and Lehtinen, K.: MATCH–SALSA – Multi-scale Atmospheric Transport and Chemistry model coupled to the SALSA aerosol microphysics model – Part 2: Sensitivity tests, Geosci. Model Dev. Discuss., in preparation, 2014.

Atkinson, R., Baulch, D. L., Cox, R. A., Crowley, J. N., Hampson, R. F., Hynes, R. G., Jenkin, M. E., Rossi, M. J., Troe, J., and IUPAC Subcommittee: Evaluated kinetic and photochemical data for atmospheric chemistry: Volume II – gas phase reactions of organic species, Atmos. Chem. Phys., 6, 3625–4055, doi:10.5194/acp-6-3625-2006, 2006.
Berge, E.,: Coupling of wet scavenging of sulphur to clouds in a numerical weather prediction model, Tellus B, 45, 1–22, 1992.
Bergman, T., Kerminen, V.-M., Korhonen, H., Lehtinen, K. J., Makkonen, R., Arola, A., Mielonen, T., Romakkaniemi, S., Kulmala, M., and Kokkola, H.: Evaluation of the sectional aerosol microphysics module SALSA implementation in ECHAM5-HAM aerosol-climate model, Geosci. Model Dev., 5, 845–868, doi:10.5194/gmd-5-845-2012, 2012.
Bergström, R., Denier van der Gon, H. A. C., Prévôt, A. S. H., Yttri, K. E., and Simpson, D.: Modelling of organic aerosols over Europe (2002–2007) using a volatility basis set (VBS) framework: application of different assumptions regarding the formation of secondary organic aerosol, Atmos. Chem. Phys., 12, 8499–8527, doi:10.5194/acp-12-8499-2012, 2012.
Carter, W. P. L.: Condensed atmospheric photooxidation mechanism for isoprene, Atmos. Environ., 30, 4275–4290, 1996.
Chamberlain, A. C. and Chadwick, R. C.: Transport of iodine from atmosphere to ground, Tellus, 18, 226–237, 1965.
Chen, Y. and Penner, J. E.: Uncertainty analysis for estimates of the first indirect aerosol effect, Atmos. Chem. Phys., 5, 2935–2948, doi:10.5194/acp-5-2935-2005, 2005.
Dana, M. T. and Hales, J. M.: Statistical aspects of the washout of polydisperse aerosols, Atmos. Environ., 10, 45–50, 1976.
Foltescu, V. L., Pryor, C. S., and Bennet, C.: Sea salt generation, dispersion and removal on the regional scale, Atmos. Environ., 39, 2123–2133, 2005.
Fountoukis, C., Racherla, P. N., Denier van der Gon, H. A. C., Polymeneas, P., Charalampidis, P. E., Pilinis, C., Wiedensohler, A., Dall'Osto, M., O'Dowd, C., and Pandis, S. N.: Evaluation of a three-dimensional chemical transport model (PMCAMx) in the European domain during the EUCAARI May 2008 campaign, Atmos. Chem. Phys., 11, 10331–10347, doi:10.5194/acp-11-10331-2011, 2011.
Gidhagen, L., Johansson, C., Langner, J., and Foltescu, V.: Urban scale modeling of particle number concentration in Stockholm. Atmos. Environ., 39, 1711–1725, 2005.
Genberg, J., Denier van der Gon, H. A. C., Simpson, D., Swietlicki, E., Areskoug, H., Beddows, D., Ceburnis, D., Fiebig, M., Hansson, H. C., Harrison, R. M., Jennings, S. G.,

Saarikoski, S., Spindler, G., Visschedijk, A. J. H., Wiedensohler, A., Yttri, K. E., and Bergström, R.: Light-absorbing carbon in Europe – measurement and modelling, with a focus on residential wood combustion emissions, Atmos. Chem. Phys., 13, 8719–8738, doi:10.5194/acp-13-8719-2013, 2013.

Gilardoni, S., Vignati, E., Cavalli, F., Putaud, J. P., Larsen, B. R., Karl, M., Stenström, K., Genberg, J., Henne, S., and Dentener, F.: Better constraints on sources of carbonaceous aerosols using a combined ^{14}C – macro tracer analysis in a European rural background site, Atmos. Chem. Phys., 11, 5685–5700, doi:10.5194/acp-11-5685-2011, 2011.

Hallquist, M., Wenger, J. C., Baltensperger, U., Rudich, Y., Simpson, D., Claeys, M., Dommen, J., Donahue, N. M., George, C., Goldstein, A. H., Hamilton, J. F., Herrmann, H., Hoffmann, T., Iinuma, Y., Jang, M., Jenkin, M. E., Jimenez, J. L., Kiendler-Scharr, A., Maenhaut, W., McFiggans, G., Mentel, Th. F., Monod, A., Prévôt, A. S. H., Seinfeld, J. H., Surratt, J. D., Szmigielski, R., and Wildt, J.: The formation, properties and impact of secondary organic aerosol: current and emerging issues, Atmos. Chem. Phys., 9, 5155–5236, doi:10.5194/acp-9-5155-2009, 2009.

Jacobson, M. Z.: Developing, Coupling and Applying a Gas, Aerosol, Transport and Radiation Model to Study Urban and Regional Air Pollution, Ph.D. thesis, Dept. of Atmospheric Sciences, University of California, Los Angeles, 1994.

Jacobson, M. Z.: Numerical techniques to solve condensational and dissolutional growth equations when growth is coupled to reversible reactions, Aerosol Sci. Tech., 27, 491–498, 1997.

Jacobson, M. Z.: Analysis of aerosol interactions with numerical techniques for solving coagulation, nucleation, condensation, dissolution, and reversible chemistry among multiple size distributions, J. Geophys. Res., 107, 4366, doi:10.1029/2001JD002044, 2002.

Jacobson, M. Z.: Fundamentals of Atmospheric Modeling, 2nd. Edn., Cambridge University Press, 2005.

Jenkin, M. E., Saunders, S. M., and Pilling, M. J.: The tropospheric degradation of volatile organic compounds: a protocol for mechanism development, Atmos. Environ., 31, 81–104, 1997.

Jönsson, O., Andersson, C., Forsberg, B., and Johansson, C.: Air pollution episodes in Stockholm regional background air due to sources in Europe and their effects on human population, Boreal Environ. Res., 18, 280–302, 2013.

Kokkola, H., Korhonen, H., Lehtinen, K. E. J., Makkonen, R., Asmi, A., Järvenoja, S., Anttila, T., Partanen, A.-I., Kulmala, M., Järvinen, H., Laaksonen, A., and Kerminen, V.-M.: SALSA – a

Sectional Aerosol module for Large Scale Applications, Atmos. Chem. Phys., 8, 2469–2483, doi:10.5194/acp-8-2469-2008, 2008.
Kuenen, J., Denier van der Gon, H., Visschedijk, A., van der Brugh, H., van Gijlswijk, R.: MACC European Emission Inventory for the Years 2003–2007, TNO Report, TNO-060-UT-2011-00588, 2011.
Kukkonen, J., Olsson, T., Schultz, D. M., Baklanov, A., Klein, T., Miranda, A. I., Monteiro, A., Hirtl, M., Tarvainen, V., Boy, M., Peuch, V.-H., Poupkou, A., Kioutsioukis, I., Finardi, S., Sofiev, M., Sokhi, R., Lehtinen, K. E. J., Karatzas, K., San José, R., Astitha, M., Kallos, G., Schaap, M., Reimer, E., Jakobs, H., and Eben, K.: A review of operational, regional-scale, chemical weather forecasting models in Europe, Atmos. Chem. Phys., 12, 1–87, doi:10.5194/acp-12-1-2012, 2012.
Kulmala, M., Lehtinen, K. E. J., and Laaksonen, A.: Cluster activation theory as an explanation of the linear dependence between formation rate of 3 nm particles and sulphuric acid concentration, Atmos. Chem. Phys., 6, 787–793, doi:10.5194/acp-6-787-2006, 2006.
Kupiainen, K. and Klimont, Z.: Primary emissions of fine carbonaceous particles in Europe, Atmos. Environ., 41, 2156–2170, 2007.
Langner, J., Bergström, R., and Pleijel, H.: European Scale Modeling of Sulfur, Oxidised Nitrogen and Photochemical Oxidants, Model Development and Evaluation for the 1994 Growing Season, SMHI RMK 82, SMHI 60176 Norrköping, Sweden, 1998.
Lee, L. A., Pringle, K. J., Reddington, C. L., Mann, G. W., Stier, P., Spracklen, D. V., Pierce, J. R., and Carslaw, K. S.: The magnitude and causes of uncertainty in global model simulations of cloud condensation nuclei, Atmos. Chem. Phys., 13, 8879–8914, doi:10.5194/acp-13-8879-2013, 2013.
Lohmann, U. and Feichter, J.: Global indirect aerosol effects: a review, Atmos. Chem. Phys., 5, 715–737, doi:10.5194/acp-5-715-2005, 2005.
Mårtensson, E. M., Nilsson, E. D., de Leeuw, G., Cohen, L. H., and Hansson, H.-C.: Laboratory simulations and parametrization of the primary marine aerosol production, J. Geophys. Res., 108, 4297, doi:10.1029/2002JD002263, 2003.
Mentel, Th. F., Wildt, J., Kiendler-Scharr, A., Kleist, E., Tillmann, R., Dal Maso, M., Fisseha, R., Hohaus, Th., Spahn, H., Uerlings, R., Wegener, R., Griffiths, P. T., Dinar, E., Rudich, Y., and Wahner, A.: Photochemical production of aerosols from real plant emissions, Atmos. Chem. Phys., 9, 4387–4406, doi:10.5194/acp-9-4387-2009, 2009.

GMDD
7, 3265–3305, 2014

Monahan, E. C., Spiel, D. E., and Davidson, K. L.: A model of marine aerosol generation via whitecaps and wave disruption, in: Oceanic Whitecaps and Their Role in Air–Sea Exchange, edited by: Monahan, E. C. and Mac Niocaill, G., D Reidel, Norwell, MA, 167–174, 1986.
Napari, I., Noppel., M., Vehkamäki, H., and Kulmala, M.: An improved model for ternary nucleation of sulfuric acid–ammonia–water, J. Chem. Phys., 116, 4221–4227, 2002a.
Napari, I., Noppel., M., Vehkamäki, H., and Kulmala, M.: Parameterization of ternary nucleation rates for H_2SO_4 – NH_3 – H_2O vapors, J. Geophys. Res., 107, 4381, doi:10.1029/2002JD002132, 2002b.
Oberdörster, G., Gelein, R., Ferin, J., and Weiss, B.: Association of particulate air pollution and acute mortality: involvement of ultrafine particles, Inhal. Toxicol., 71, 111–124, 1995.
O'Dowd, C. D., Facchini, M. C., Cavalli, F., Ceburnis, D., Mircea, M., Decesari, S., Fuzzi, S., Yoon, Y. J., and Putaud, J.-P.: Biogenically driven organic contribution to marine aerosol, Nature, 431, 676–680, 2004.
Paasonen, P., Nieminen, T., Asmi, E., Manninen, H. E., Petäjä, T., Plass-Dülmer, C., Flentje, H., Birmili, W., Wiedensohler, A., Hõrrak, U., Metzger, A., Hamed, A., Laaksonen, A., Facchini, M. C., Kerminen, V.-M., and Kulmala, M.: On the roles of sulphuric acid and low-volatility organic vapours in the initial steps of atmospheric new particle formation, Atmos. Chem. Phys., 10, 11223–11242, doi:10.5194/acp-10-11223-2010, 2010.
Peters, A., Wichmann, E., Tuch, T., Heinrich, J., and Heyder, J.: Respiratory effects are associated with the number of fine particles, Am. J. Resp. Crit. Care, 155, 1376–1383, 1997.
Pope, C. A. and Dockery, D. W.: Health effects of fine particulate air pollution: lines that connect, JAPCA J. Air Waste Ma., 56, 709–741, 2006.
Pouliot, G., Thomas Pierce, T., Denier van der Gon, H., Schaap, M., Moran, M., and Nopmongcol, U.: Comparing emission inventories and model-ready emission datasets between Europe and North America for the AQMEII project, Atmos. Environ., 53, 4–14, 2012.
Reddington, C. L., Carslaw, K. S., Spracklen, D. V., Frontoso, M. G., Collins, L., Merikanto, J., Minikin, A., Hamburger, T., Coe, H., Kulmala, M., Aalto, P., Flentje, H., Plass-Dülmer, C., Birmili, W., Wiedensohler, A., Wehner, B., Tuch, T., Sonntag, A., O'Dowd, C. D., Jennings, S. G., Dupuy, R., Baltensperger, U., Weingartner, E., Hansson, H.-C., Tunved, P., Laj, P., Sellegri, K., Boulon, J., Putaud, J.-P., Gruening, C., Swietlicki, E., Roldin, P., Henzing, J. S., Moerman, M., Mihalopoulos, N., Kouvarakis, G., Ždímal, V., Zíková, N., Marinoni, A., Bonasoni, P., and Duchi, R.: Primary versus secondary contributions to particle number concentrations in

GMDD
7, 3265–3305, 2014

MATCH–SALSA – Part 1: Model description and evaluation

C. Andersson et al.

the European boundary layer, Atmos. Chem. Phys., 11, 12007–12036, doi:10.5194/acp-11-12007-2011, 2011.
Riipinen, I., Sihto, S.-L., Kulmala, M., Arnold, F., Dal Maso, M., Birmili, W., Saarnio, K., Teinilä, K., Kerminen, V.-M., Laaksonen, A., and Lehtinen, K. E. J.: Connections between atmospheric sulphuric acid and new particle formation during QUEST III–IV campaigns in Heidelberg and Hyytiälä, Atmos. Chem. Phys., 7, 1899–1914, doi:10.5194/acp-7-1899-2007, 2007.
Robertson, L., Langner, J., and Engardt, M.: An Eulerian limited-area atmospheric transport model, J. Appl. Meteorol., 38, 190–210, 1999.
Roesler, E. L. and Penner, J. E.: Can global models ignore the chemical composition of aerosols?, Geophys. Res. Lett., 17, L24809, doi:10.1029/2010GL044282, 2010.
Saunders, S. M., Jenkin, M. E., Derwent, R. G., and Pilling, M. J.: Protocol for the development of the Master Chemical Mechanism, MCM v3 (Part A): tropospheric degradation of non-aromatic volatile organic compounds, Atmos. Chem. Phys., 3, 161–180, doi:10.5194/acp-3-161-2003, 2003.
Schlesinger, R. B., Kunzli, N., Hidy, G. M., Gotschi, T., and Jerrett, M.: The health relevance of ambient particulate matter characteristics: coherence of toxicological and epidemiological inferences, Inhal. Toxicol., 18, 95–125, 2006.
Seinfeld, J. H. and Pandis, S. N.: Atmospheric Chemistry and Physics: from Air Pollution to Climate Change, John Wiley and Sons, 1997.
Simon, H., Bhave, P. V., Swall, J. L., Frank, N. H., and Malm, W. C.: Determining the spatial and seasonal variability in OM/OC ratios across the US using multiple regression, Atmos. Chem. Phys., 11, 2933–2949, doi:10.5194/acp-11-2933-2011, 2011.
Simpson, D.: Long-period modelling of photochemical oxidants in Europe. Model calculations for July 1995, Atmos. Environ., 26A, 1609–1634, 1992.
Simpson, D., Andersson-Sklöld, Y., and Jenkin, M. E.: Updating the Chemical Scheme for the EMEP MSC-W Oxidant Model: Current Status, EMEP MSC-W Note 2/93, 1993.
Simpson, D., Guenther, A., Hewit, C. N., and Steinbrecher, R.: Biogenic emissions in Europe. 1. Estimates and uncertainties, J. Geophys. Res., 100, 22875–22800, 1995.
Simpson, D., Yttri, K., Klimont, Z., Kupiainen, K., Caseiro, A., Gelencsér, A., Pio, C., and Legrand, M.: Modeling carbonaceous aerosol over Europe. Analysis of the CARBOSOL and EMEP EC/OC campaigns, J. Geophys. Res., 112, D23S14, doi:10.1029/2006JD008158, 2007.

Simpson, D., Benedictow, A., Berge, H., Bergström, R., Emberson, L. D., Fagerli, H., Flechard, C. R., Hayman, G. D., Gauss, M., Jonson, J. E., Jenkin, M. E., Nyíri, A., Richter, C., Semeena, V. S., Tsyro, S., Tuovinen, J.-P., Valdebenito, Á., and Wind, P.: The EMEP MSC-W chemical transport model – technical description, Atmos. Chem. Phys., 12, 7825–7865, doi:10.5194/acp-12-7825-2012, 2012.

Spracklen, D. V., Pringle, K. J., Carslaw, K. S., Chipperfield, M. P., and Mann, G. W.: A global off-line model of size-resolved aerosol microphysics: II. Identification of key uncertainties, Atmos. Chem. Phys., 5, 3233–3250, doi:10.5194/acp-5-3233-2005, 2005.

Spracklen, D. V., Carslaw, K. S., Merikanto, J., Mann, G. W., Reddington, C. L., Pickering, S., Ogren, J. A., Andrews, E., Baltensperger, U., Weingartner, E., Boy, M., Kulmala, M., Laakso, L., Lihavainen, H., Kivekäs, N., Komppula, M., Mihalopoulos, N., Kouvarakis, G., Jennings, S. G., O'Dowd, C., Birmili, W., Wiedensohler, A., Weller, R., Gras, J., Laj, P., Sellegri, K., Bonn, B., Krejci, R., Laaksonen, A., Hamed, A., Minikin, A., Harrison, R. M., Talbot, R., and Sun, J.: Explaining global surface aerosol number concentrations in terms of primary emissions and particle formation, Atmos. Chem. Phys., 10, 4775–4793, doi:10.5194/acp-10-4775-2010, 2010.

Stern, R., Builtjes, P., Schaap, M., Timmermans, R., Vautard, R., Hodzic, A., Memmesheimer, M., Feldmann, H., Renner, E., Wolke, R., and Kerschbaumer, A.: A model inter-comparison study focussing on episodes with elevated PM_{10} concentrations, Atmos. Environ., 42, 4567–4588, doi:10.1016/j.atmosenv.2008.01.068, 2008.

Turpin, B. J., Saxena, P., and Andrews, E.: Measuring and simulating particle organics in the atmosphere: problems and prospects, Atmos. Environ., 38, 2983–3013, 2000.

Undén, P., Rontu, L., Järvinen, H., Lynch, P., Calvo, J., Cats, G., Cuxart, J., Eerola, K., Fortelius, C., Garcia-Moya, J. A., Jones, C., Lenderlink, G., Mcdonald, A., Mcgrath, R., Navascues, B., Nielsen, N. W., Degaard, V., Rodriguez, E., Rummukainen, M., Sattler, K., Hansen Sass, B., Savijarvi, H., Wichers Schreur, B., and Sigg, R.: The HIRLAM-5 Scientific Documentation, available at: http://www.hirlam.org (last access: 6 May 2014), 2002.

Vehkamaki, H., Kulmala, M., Napari, I., Lehtinen, K. E. J., Timmreck, C., Noppel, M., and Laaksonen, A.: An improved parameterization for sulphuric acid/water nucleation rates for tropospheric and stratospheric conditions, J. Geophys. Res., 107, 4622, doi:10.1029/2002LD002184, 2002.

Visschedijk, A. J. H., Denier van der Gon, H., A. C., Dröge, R., Van der Brugh, H., Kooter, I. M.,: A European High Resolution and Size-Differentiated Emission Inventory for Elemental and Organic Carbon for the Year 2005, TNO report, TNO-034-UT-2009-00688-RPT-ML, 2009.

Yu, F. and Luo, G.: Simulation of particle size distribution with a global aerosol model: contribution of nucleation to aerosol and CCN number concentrations, Atmos. Chem. Phys., 9, 7691–7710, doi:10.5194/acp-9-7691-2009, 2009.

Zhang, L., Gong, S., Padro, J., and Barrie, L.: A size-segregated particle dry deposition scheme for an atmospheric aerosol module, Atmos. Environ., 35, 549–560, 2001.

GMDD

7, 3265–3305, 2014

MATCH–SALSA – Part 1: Model description and evaluation

C. Andersson et al.

Table 1. Comparison of modeled secondary inorganic aerosol (SIA) components to daily observed concentrations. Average results covering available measurements for the year 2007 (results for individual stations are given in the Supplement Tables A15–A19). In addition to the SIA components also the total nitrate ($TNO_3 = HNO_3(g) + NO_3^-(p)$) and total reduced nitrogen ($TNH_x = NH_3(g) + NH_4^+(p)$) are evaluated.

	Global/temporal						Spatial			
Measure:	Mean Obs	Mean Mod	%Bias	mean[a] r	mean[a] CV(RMSE)	#obs	%Bias	r	CV(RMSE)	#stns
Unit:	$\mu g\,S/N\,m^{-3}$	$\mu g\,S/N\,m^{-3}$	%		%		%		%	
SO_4^{2-}	0.63	0.65	4	0.52	46	16 033	−6	0.57	53	52
NO_3^-	0.40	0.32	−21	0.44	49	7249	−22	0.83	48	23
TNO_3	0.49	0.40	−19	0.59	36	11 039	−21	0.85	41	35
NH_4^+	0.72	0.64	−12	0.57	39	9728	−11	0.79	37	31
TNH_x	1.27	1.01	−21	0.53	40	10 137	−20	0.87	38	32

[a] Weighted average of correlation coefficients and CV(RMSE) at individual stations.

GMDD
7, 3265–3305, 2014

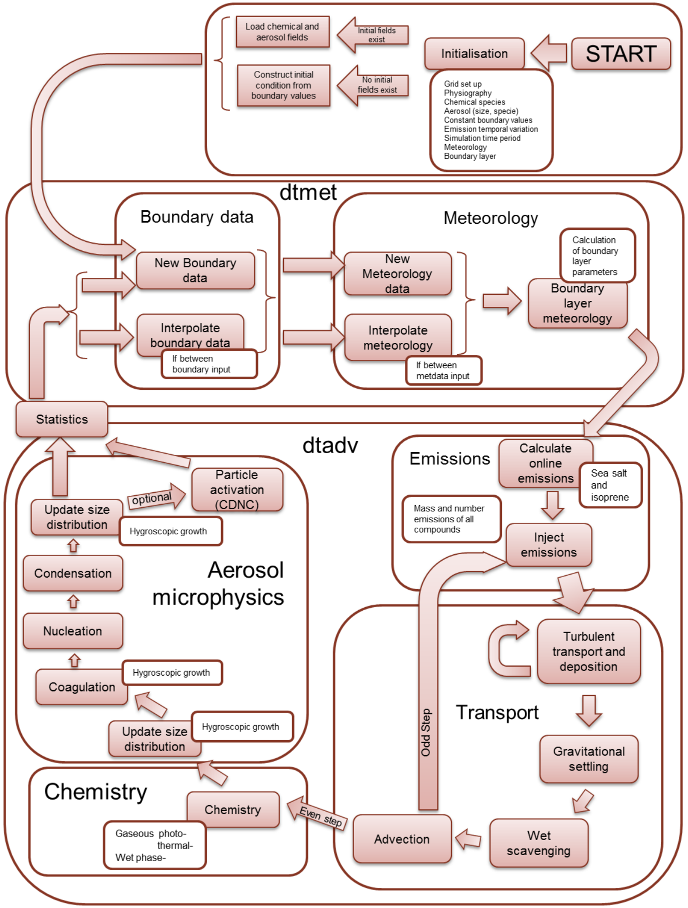

Fig. 1. Data flow and time stepping in MATCH–SALSA.

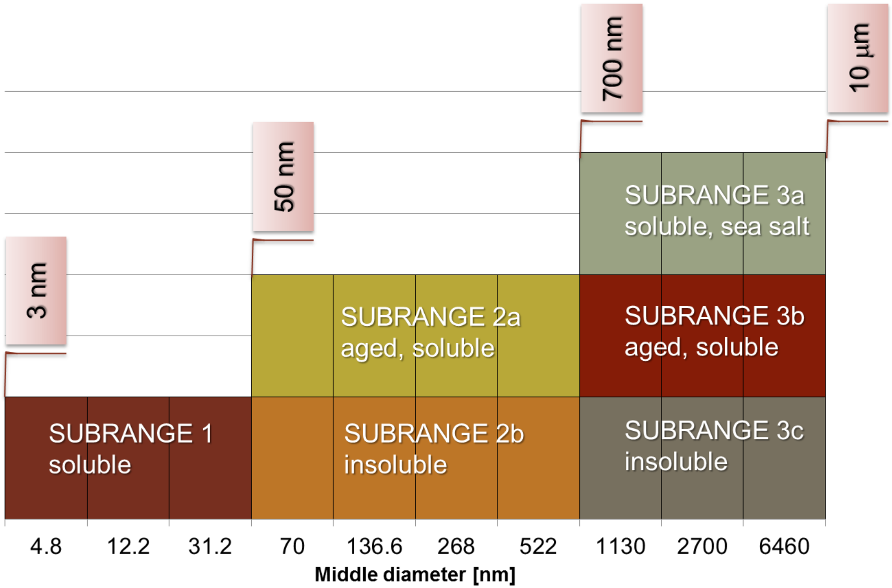

Fig. 2. Aerosol division into bins in the three SALSA subranges in the base case set up of MATCH–SALSA.

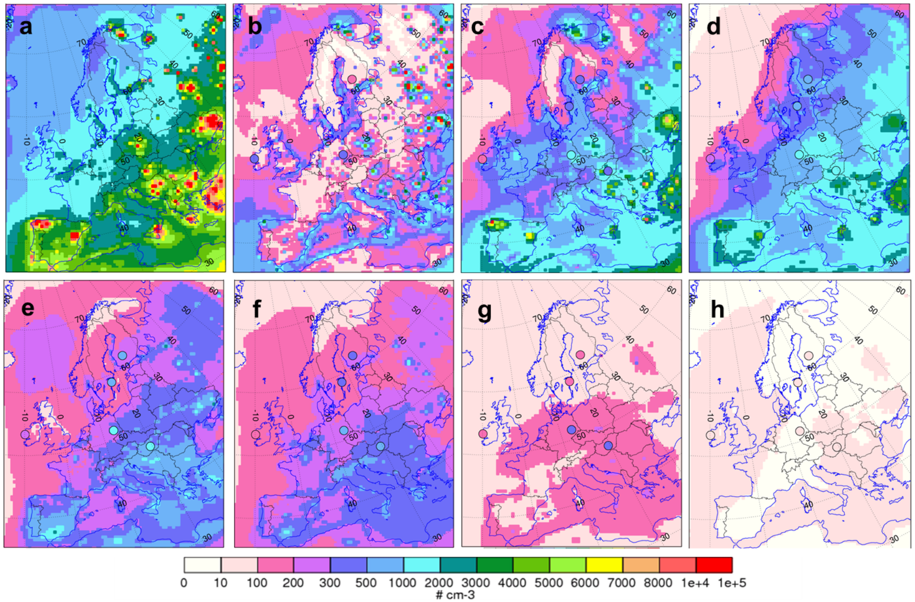

Fig. 3. Calculated annual mean (2007) particle number concentration (PNC) in Europe. Total PNC (sum of all sizes; **a**), and PNC in size bins $\mathrm{PNC}_{3<d<7\,\mathrm{nm}}$ **(b)**, $\mathrm{PNC}_{7<d<20\,\mathrm{nm}}$ **(c)**, $\mathrm{PNC}_{20<d<50\,\mathrm{nm}}$ **(d)**, $\mathrm{PNC}_{50<d<98\,\mathrm{nm}}$ **(e)**, $\mathrm{PNC}_{98<d<192\,\mathrm{nm}}$ **(f)**, $\mathrm{PNC}_{192<d<360\,\mathrm{nm}}$ **(g)**, $\mathrm{PNC}_{360<d<700\,\mathrm{nm}}$ **(h)**. Observed annual mean PNC (filled circles) at the observation sites: Hyytiälä (Finland), Aspvreten (Sweden), Melpitz (Germany), K-Puszta (Hungary) and Mace Head (Ireland) when observed numbers exist in the indicated interval. Unit: $\#\,\mathrm{cm}^{-3}$.

GMDD
7, 3265–3305, 2014

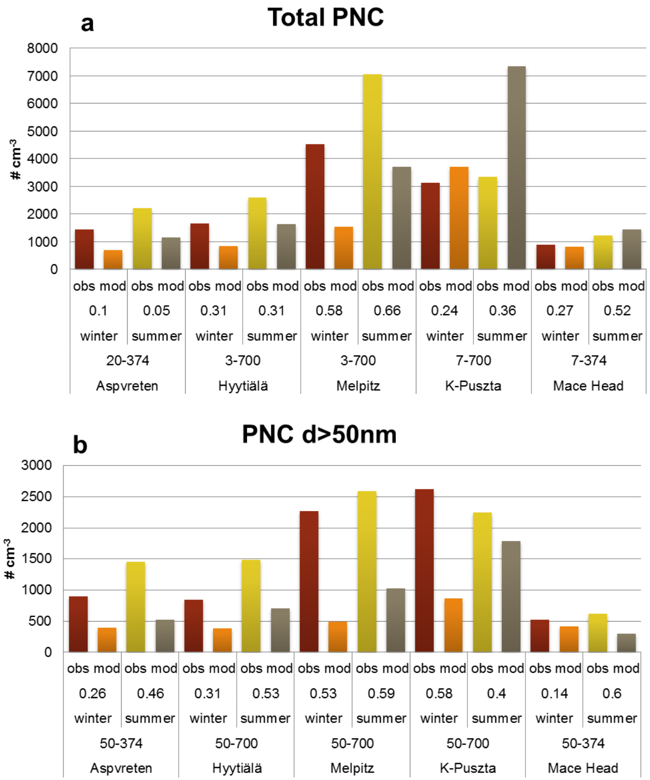

Fig. 4. Mean particle number concentration (PNC) in winter and summer at five observation sites in Europe. Top panel **(a)**: mean observed and modeled total PNC. Bottom panel **(b)**: mean observed and modeled PNC in the accumulation mode. The interval above the observation site name indicates the particle size interval included, unit nm. The number above the season indication shows the (Pearson) correlation coefficient of daily mean PNC. Note that the size intervals differ between the stations: the size interval is used for both modeled and observed values. Unit: # cm^{-3}.

GMDD
7, 3265–3305, 2014

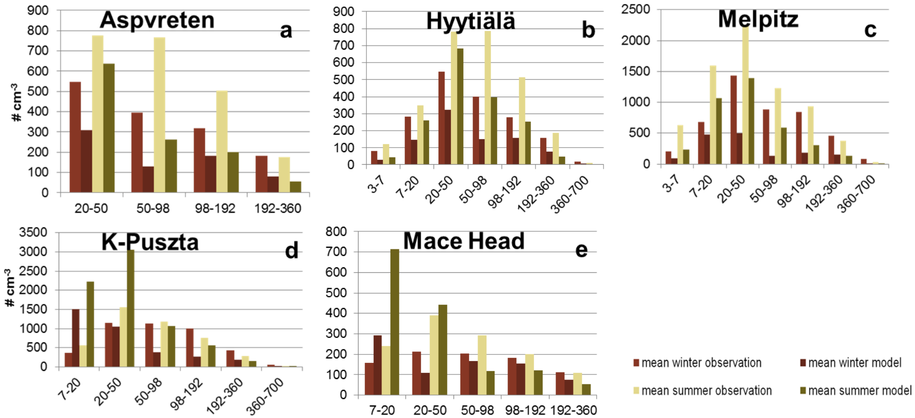

Fig. 5. Modeled and measured winter (January–March, October–December) and summer (April–September) mean particle number concentration size distribution at five measurement sites in Europe during 2007. Unit: # cm^{-3}.

GMDD
7, 3265–3305, 2014

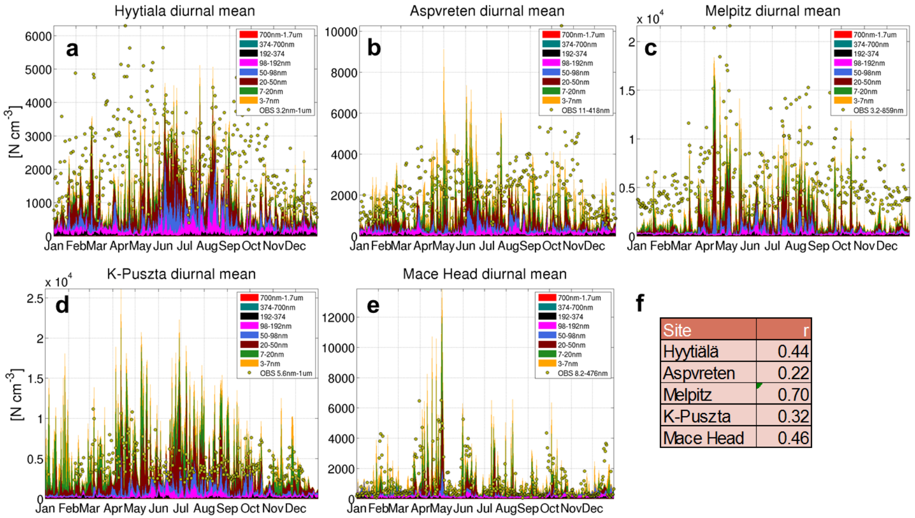

Site	r
Hyytiälä	0.44
Aspvreten	0.22
Melpitz	0.70
K-Puszta	0.32
Mace Head	0.46

Fig. 6. Observed and modeled daily mean particle number concentrations (PNC) at five sites in Europe during 2007 **(a–e)**. Modeled (surfaces) and observed (filled circles) daily mean PNC in size bins are displayed as a time series. See legend for colors representing the different size bins. Unit: # cm^{-3}. **(f)** (Pearson) correlation coefficient for evaluation of diurnal means during 2007.

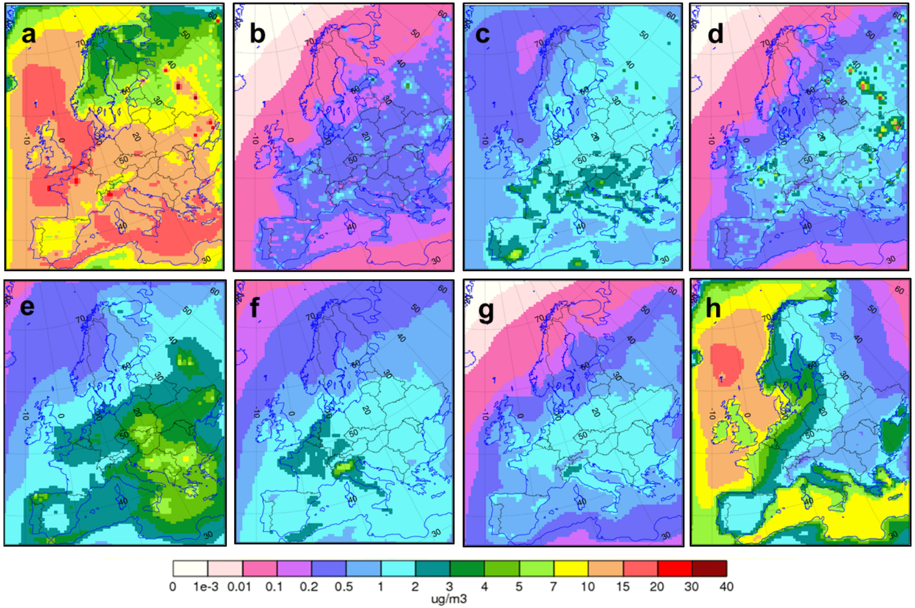

Fig. 7. Modeled annual mean concentrations (for 2007) of PM_{10} (**a**; peak at 37 $\mu g\,m^{-3}$ in Moscow) and its particle components: elemental carbon **(b)**, organic matter **(c)**, anthropogenic primary inorganic aerosol **(d)**, sulfate **(e)**, nitrate **(f)**, ammonium **(g)** and sea salt **(h)**. Unit: $\mu g\,m^{-3}$.

GMDD
7, 3265–3305, 2014

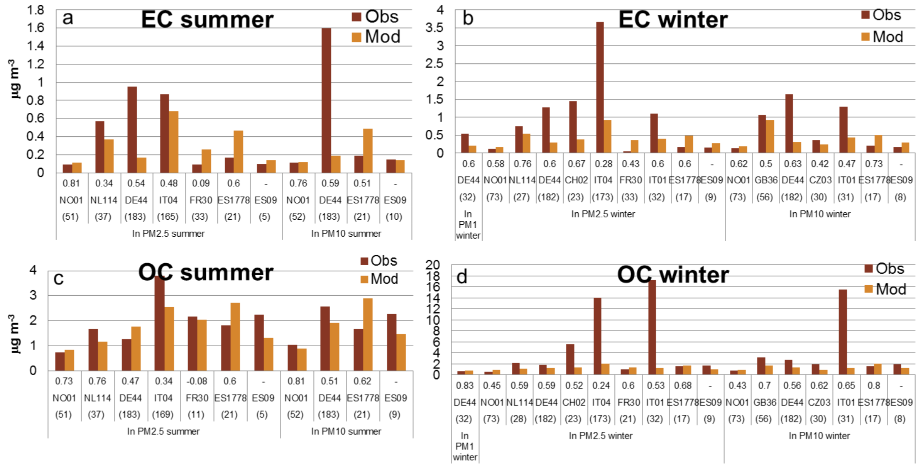

Fig. 8. Evaluation of EC (top row **a**: April–September mean; **b**: October–March mean) and OC (bottom **c**: April–September mean; **d**: October–March mean) for 2007. Observed and modeled mean concentrations (unit: $\mu g\,m^{-3}$), correlation coefficients of daily mean concentrations are indicated below the bars. The number of daily mean values is indicated by the numbers in the parentheses. Correlation coefficients were calculated for measurement sites with more than 10 daily observations. Site codes as defined by EMEP, see Supplement Table 5.

GMDD
7, 3265–3305, 2014

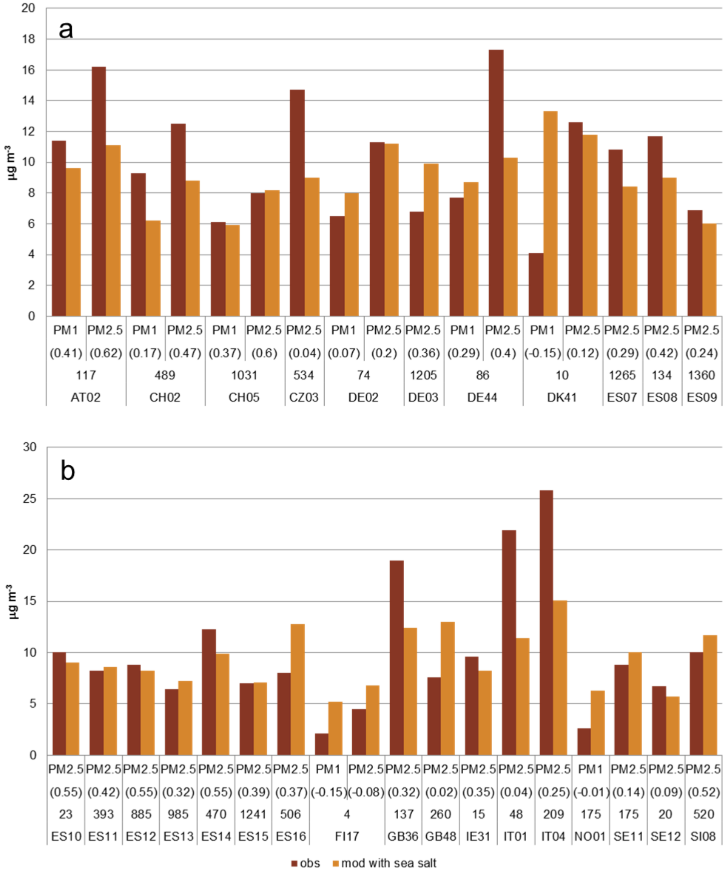

Fig. 9. Evaluation of PM_1 and $PM_{2.5}$ for 2007. Observed and modeled mean concentrations (unit: $\mu g\,m^{-3}$); correlation coefficients of daily mean concentrations are indicated below the bars within parentheses. The elevation of each site is included below the correlation coefficients (unit: m a.s.l.). Station codes as defined by EMEP, see Supplement Table 5.

GMDD
7, 3265–3305, 2014